

Sub-6 GHz Millimeter-Wave Metamaterial Antenna with Reconfigurable Radiation Patterns for Enhanced Wireless Communication

Abubakar LAWAL¹, Abdulkadir O. ABDULBAKI^{2*}, Nathaniel SALAWU³, Bala A. SALIHU⁴, Mamman A. THOMAS⁵, Abraham U. USMAN⁶

^{1,2,3,4,5,6}Department of Telecommunications Engineering, Federal University of Technology, Minna, Nigeria

³Department of Electrical and Electronics Engineering, Confluence University of Science and Technology, Osara, Kogi State, Nigeria

¹abubakarlawal@st.futminna.edu.ng, ^{2*}abdulkadir.abdulkaki@futminna.edu.ng, ³nathanielsalawu@futminna.edu.ng,

⁴salbala@futminna.edu.ng, ⁵thomas.mamman@futminna.edu.ng, ⁶usman.abraham@futminna.edu.ng

Abstract

6G has been envisioned to utilize the upper mmWave (90-300 GHz) and Terahertz bands (0.1-10 THz). At such high frequencies, high path loss and atmospheric absorption are critical challenges. A highly directional and reconfigurable antenna is required to mitigate these challenges. This research presents a novel, pattern-reconfigurable metamaterial-based antenna for sub-6 GHz mmWave applications. The antenna is based on a graphene metasurface loaded with a novel square-spherical split ring resonator, positioned above a rectangular microstrip patch antenna to provide absorption of unwanted signals and improve gain and spectral efficiency. Placed under the patch is Rogers 5800 substrate with permittivity (ϵ) of 2.0 and thickness of 0.1 mm. The antenna operates between 90-120 GHz, spanning the 102-109 GHz, adopted at the World Radio Congress 2023 for advanced use cases of 6G, and was simulated using the CST suite. The main beam is pattern-reconfigured by two bipolar junction diodes (d_1 , d_2) embedded on the patch antenna. The diodes reconfigure the radiation pattern and affect the S_{11} reflection coefficient. Specifically, d_1 switches between 90-98 GHz, obtaining a minimum S_{11} of -70.7 dB at 97.5 GHz, while d_2 switches between 98-120 GHz, realizing a minimum S_{11} of -69.6 dB at 105.4 GHz. When fully loaded, a -64.5 dB was obtained, better than similar work compared. These S_{11} values indicate exceptional impedance matching and minimal signal reflection. The proposed antenna introduces a novel design that integrates a square-spherical split ring resonator with a graphene metasurface, achieving dynamic pattern reconfigurability and deep S_{11} nulls in a compact structure. The antenna is compact, has a wide bandwidth, and can perform efficiently in 6G use cases, including holographic presence, and smart transport, among others require high radiation efficiency. Real-world use cases include holographic presence, smart mobility, and on-chip THz systems, where beam reconfigurability and low reflection loss are critical.

Keywords: 6G Antenna, Metamaterial, mmWave, Terahertz band, split ring.

1.0 Introduction

The evolution of wireless communication from analog telephone systems to today's broadband connectivity has opened the door for new, data-intensive applications such as holographic presence, ultra-HD video, and tactile internet. With the number of connected devices projected to exceed 90 billion by 2030 [1], current wireless technologies are fast approaching their performance limits. The sixth generation (6G) of wireless communication is emerging as a revolutionary solution, offering ultra-reliable, low-latency, and high-efficiency connectivity to support these advanced use cases [2].

At the World Radio Conference (WRC) 2023, the International Telecommunication Union (ITU)-R allocated new frequency bands for 6G communication, spanning from 4.4 GHz to 14.8 GHz for general mobile use, and 102 GHz to 278 GHz for advanced applications [3]. To support communication at such high frequencies, wireless devices must become more compact, efficient, and reliable—placing significant demands on their antenna systems. Antennas, which serve as the interface between guided and free-space electromagnetic waves [4], must now be reimagined to meet these new requirements.

As communication shifts to the sub-terahertz (sub-THz) and THz frequency bands, traditional antenna designs face challenges such as high path loss and atmospheric absorption. These issues require antennas that are not only highly directional but also reconfigurable. Existing solutions, including those based on square split ring (SSR) resonators, often demand complex, multilayered implementations. To address these limitations, this project proposes the design of a square split-spherical ring (SSSR) reconfigurable metamaterial antenna capable of operating between 90 GHz and 120 GHz.

The motivation behind this study stems from the growing need for intelligent, compact antenna systems that can adapt their transmission patterns in real time to minimize signal degradation. The proposed antenna is designed using the CST Studio Suite and aims to achieve spectral efficiency by dynamically reorienting itself toward the strongest available signal direction. The antenna was rigorously evaluated based on performance parameters

such as reflection coefficient, bandwidth, and refractive index, and its effectiveness was also validated through comparison with existing designs.

The success of this study depends on the antenna's ability to deliver high gain, broad bandwidth, and adaptive reconfigurability all of which are crucial to overcoming the inherent limitations of high-frequency communication.

The major contribution of this work is that the study presents a new Square-Spherical Split Ring (SSSR) metamaterial-based antenna for sub-6G mmWave applications, addressing key challenges in 6G communications. The design integrates a graphene metasurface with a PIN diode-driven reconfigurable patch antenna, enabling dynamic four-directional beam steering in the 90-120 GHz band. The SSSR unit cell achieves a wide bandwidth and dual-band operation with an exceptional reflection coefficient of -64.5 dB. The antenna's near-zero refractive index enhances beamforming efficiency, and its compact Rogers 5800 substrate minimizes loss. This design offers superior gain, reconfigurability, and spectral efficiency, making it ideal for 6G applications.

2.0 Related Works

The challenge of high path loss and atmospheric absorption at mmWave has led researchers to design different antenna structures to mitigate the losses. The authors [5] designed a Rectangular Split Ring Resonator (RSRRs) reconfigurable antenna using the CST suite. The presented design has a simplified geometry with dimensions $30 \times 22 \times 1.6 \text{ mm}^3$, and could be reconfigured to other desired frequencies by modification of the PIN diodes and the dimensions of the RSRRs and across the circular patch antenna.

An ultra-wideband (UWB) reconfigurable mmWave/THz microstrip antenna with two PIN diodes mounted on a benzocyclobutene polymer and a novel gold radiating patch was presented in another study by [6]. For the ON and OFF states of the PIN diodes deployed, the equivalent resistor (R), capacitor (C), and inductor (L) were, respectively, 100 pH, 4 fF, and 10 ohms. Using frequency reconfiguration, the antenna achieved an 8.59 dB gain while operating in the 100–303 GHz range.

A metasurface antenna with optically controlled radiation properties by PIN photodiodes was proposed by [7]. With a reflection coefficient (S11) greater than -10 dB and a peak gain of 9 dBi at 1.35 GHz, the antenna works between 0.978 GHz and 1.73 GHz. The proposed antenna consists of a standard rectangular patch with a slot for an order 3 H-tree fractal embedded in it. There is a tiny air gap between the patch radiator and the metasurface layer it is positioned atop. The antenna reconfiguration is made possible by the PIN photodiodes that link the unit cells in the lattice structure that makes up the metasurface layer.

The authors [8] proposed a high-gain circularly polarised (CP) antenna with an MNG metamaterial slab and NRZI (Near Zero Refractive Index). MNG (Mu Negative) metamaterial slab and Refractive Index. To attain high gain and circular polarisation, the antenna used a substrate-integrated waveguide (SIW) approach loaded with a small SSR resonator combined with a shape that has hexagonal structure of a 0.2 mm width slab as a unit cell. The antenna was simulated across a broad range of frequencies, between 100GHz to 280GHz, recording maximum 11.3dB gain at 223GHz. Although high gain and good cross-polarization were achieved, the antenna was not reconfigurable type.

The authors [9] designed an antenna for 6G applications, which has dimensions of 30 mm x 20 mm x 1.6 mm and is built on FR-4 material with a relative permittivity of $\epsilon_r = 4.4$. The design allows for three operation modes: mode 1 (SW1= Off and SW2= Off) covering a 4.6 GHz band, mode 2 (SW1= On, SW2= Off or SW1=Off, SW2=On), and mode 3 (SW1= On, SW2= On). The design module's dimensions and performance are suitable, demonstrating its practicality. However, the main disadvantages of the design are interference, fading, multipath, and switch mismatching.

In the work of [10], the authors present an analytical design of a new compact coplanar waveguide (CPW) fed ultra-wideband (UWB) antenna operable in the spectrum between 23–150 GHz. It exhibits remarkable performance in the mm-Wave Spectrum with simulated radiation efficiency over 90% and gain over 4.5 dBi in the entire band. Moreover, with a 147.2% fractional bandwidth, this newly proposed miniaturized antenna ($17 \times 15 \times 0.787 \text{ mm}^3$) is envisaged to be deployed for the higher band of 5G as well as the next generation 6G wireless communication.

3.0 Methodology

6G is at the design and testing stage. Within the scope of this work to design an antenna that meets the requirements for 6G antennas (reconfigurability, high gain, and wide bandwidth), the CST suite has been utilized. The antenna is designed following Figure 1.

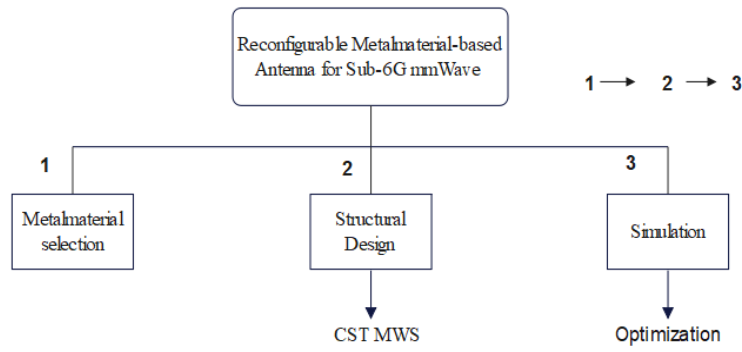


Figure 1: Design steps

3.1 Proposed System

In the field of electromagnetism, materials are either homogeneous or non-homogeneous. Homogeneous materials are defined by their constituent intrinsic parameters such as permittivity (ϵ) and permeability (μ), while non-homogeneous materials, such as Metamaterials (MMs), are defined by effective (ϵ) and (μ). Let the effective permittivity, permeability, and refractive index [11].

3.2 Antenna Structure Design

1) Unit Cell Design

The final metamaterial's properties are largely determined by the shape of the unit cell. From the literature, the fishnet structures, mushroom structures, or split ring resonators have been generally adopted; however, in this work, a square-spherical split ring (SSSR) has been presented.

In order to create a metamaterial, a unit cell must first be created. This will allow for the necessary propagation properties, such as strong absorption, negative-refractive index, negative (ϵ), and positive (μ), to be achieved. Figure 2 shows how the suggested unit cell has evolved. In CST MWS, the unit cell has been developed and modelled to function in the sub-mmWave frequency range of 90GHz to 120GHz. Table 1 contains the unit cell's measurements.

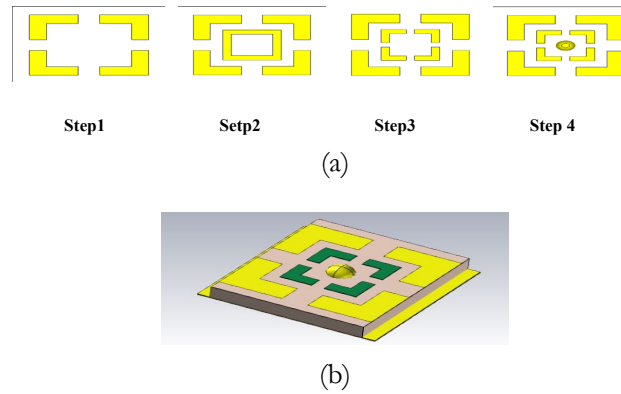


Figure 2: (a) Evolution of square spherical split ring (SSSR) unit cell (b) Proposed SSSR

Table 1: Antenna design parameters

Parameter	Unit (mm)	Representation
L	0.6	Length of the patch
W	1.11	Width of the patch
f_g	0.10	Feed line gap
t_s	0.05	Thickness of the substrate
L	0.8	Length of unit cell
W	0.8	Width of unit cell
t_g	0.8	Unit cell ground thickness
Re1	0.2	Outer square ring cut
Re2	0.08	Inner square ring cut
c_t	0.02	Thickness of the spherical ring
R	0.6	Radius of the spherical ring

2) Pattern Reconfigurable SSSR Metamaterial Antenna Design

A pattern reconfigurable metamaterial antenna was designed as depicted in Figure 3. The antenna structure consists of six parts, which include, ground, substrate, SSSR graphene surface, antenna radiating structure, PIN diode, and feedline.

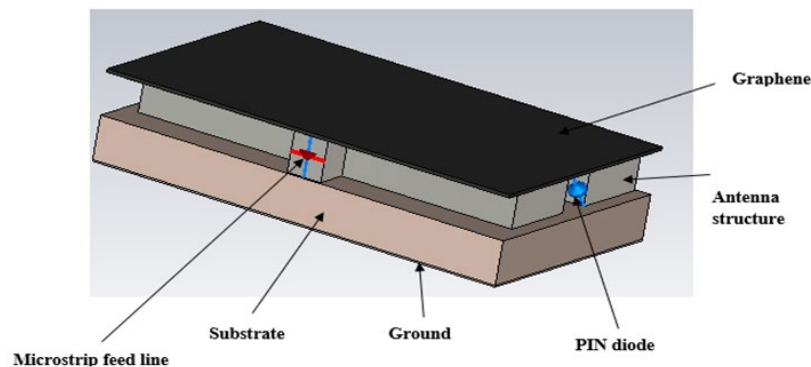


Figure 3: Structural design of 6G reconfigurable antenna

The designed antenna structure was based on a graphene metamaterial placed above the patch antenna to provide absorption of unwanted signals, improve gain, and spectral efficiency. The metasurface layer comprises a 5×7 SSSR unit-cell matrix. The length and width of each unit cell are 0.8mm. There is a 2 mm space between subsequent unit cells. Integrated PIN diodes (d1, d2) in the patch antenna reconfigure the main beam. Placed under the patch is Rogers 5800 substrate with permittivity (ϵ) of 2.0 and thickness of 0.1mm, and a reflective annealed copper that reduces radiation coming from the patch's back. This is essential for increasing the antenna's front-to-back ratio. Pattern reconfiguration is achieved by the PIN diodes (d1 and d2), which switch according to the current distribution on the metasurface. The antenna is fed through a 50Ω microstrip line.

The antenna was modeled and simulated using CST Microwave Studio. Two main simulation types were used to evaluate its performance. First, frequency-domain analysis was performed to extract the S-parameters, especially the S11 reflection coefficient, across the target band of 90–120 GHz. This directly supports the S11 results presented later, including the deep nulls at 97.5 GHz, 105.4 GHz, and 102.17 GHz. Secondly, parameter sweeps were used to simulate the ON/OFF states of the two PIN diodes (d1 and d2), modeling their influence on bandwidth, gain, and pattern reconfiguration. These simulations collectively confirmed the antenna's performance as presented in the result sections.

Graphene, used in the metasurface layer, plays a crucial role in the reconfigurability and performance of the antenna. Its electrical conductivity is tunable by applying an external voltage bias, which allows dynamic control of surface current distribution and thereby real-time beam redirection. Furthermore, graphene has a low loss tangent in the sub-terahertz frequency range, which significantly reduces dielectric loss and enhances radiation efficiency. These properties make graphene highly suitable for sub-THz metamaterial antennas and directly support the deep S11 values and beam steering performance [7].

Two PIN diodes, d1 and d2 perform pattern reconfiguration of the beam incident on the metasurface. The dimensions of the rectangular patch antenna are obtained from [7]. The evolution of the antenna structure is shown in Figure 4. Antenna1 is the rectangular patch with two cuts at strategic positions to allow for the interconnection of the diodes. Antenna2 is PIN diode enabled, while Antenna3 is the full antenna structure loaded with SSSR-metasurface. Table 1 displays the dimensions of the designed antenna.

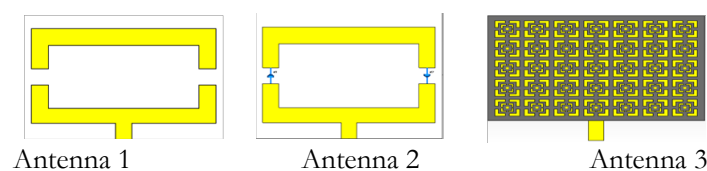


Figure 4: Evolution of the antenna and simulation set-up

3.3 Antenna Reconfiguration

An antenna's spatial dispersion of radiation field is directly influenced by its current orientation. The antenna's radiation pattern can be changed without changing its frequency by utilizing the relationship between the source current and the radiation field, resulting in a reconfigurable pattern design [12]. An antenna is pattern reconfigured by changing the metasurface layer's characteristics [13]. This was achieved in this work by inter-switching the PIN

diodes d1 and d2 as shown in Figure 5. d1 with respect to the magnetic radiation incident on the metasurface plane. The metamaterial provides maximum directivity along the axis with more current density.

The two diodes (d1, d2) employed in this research work are BAR50-02L PIN. According to the datasheet, the diode is equivalent to a series RLC ($R = 4\Omega$, $L=C=0$) for the ON state and a parallel RLC ($R=5\text{ k}\Omega$, $L = 0$, $C = 0.07\text{ pF}$) for the OFF state. The justification for PIN switching includes high isolation between on and off states, low insertion loss, fast switching time, and low power consumption. Additionally, it can easily be implemented using a simple biasing circuit, it allows for flexible control over the antenna's radiation pattern and is relatively low in cost compared to other switching techniques.

4.0 Results and Discussion

4.1 Metamaterial Unit Cell Result

The S11 plot along the x-axis at each stage of the unit cell design evolution is illustrated in Figure 5. The S11 parameter depicts the reflection coefficient of an antenna, indicating the radiation of useful power.

In stage1, the $S_{11} \leq -10\text{ dB}$ is not satisfied as the resonator performs poorly. A 2.55 GHz single-bandwidth is however, realized in stage2 with acceptable return loss. The unit cell performs better in stage4, realizing a wide bandwidth of 11.77 GHz, an $S_{11} \leq -10\text{ dB}$ of -25.35 dB, and a double band (91.27-93.58 GHz and 101.17-112.94 GHz) operation. Along the z-axis, the S12 plot of the unit-cell was displayed in Figure 6. The antenna exhibits peak radiation at 118 GHz.

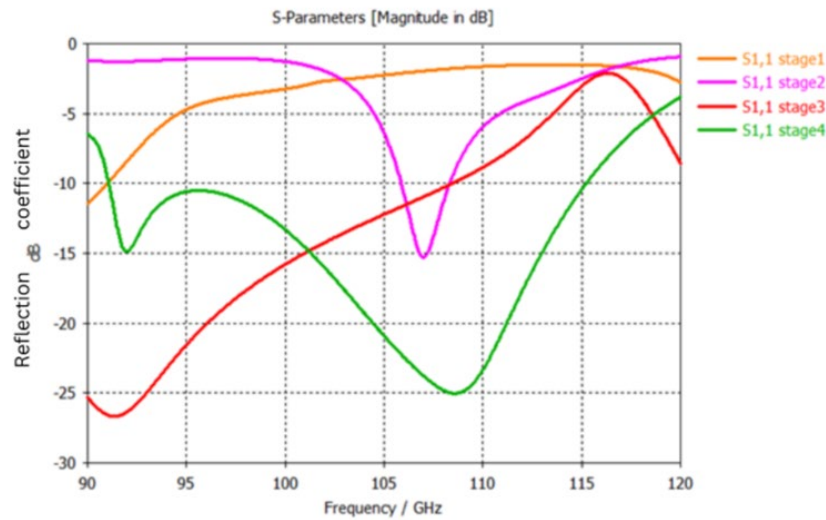


Figure 5: S11 Results of SSSR metamaterial unit cell along the x-axis

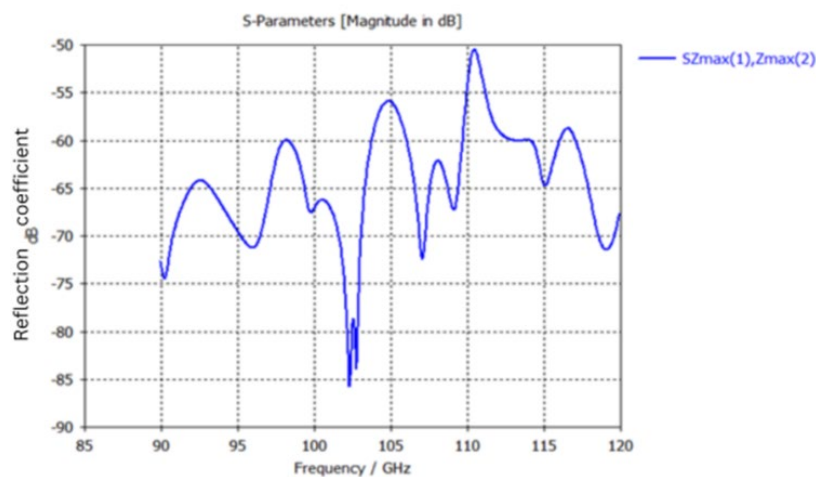


Figure 6: S12 of SSSR unit cell along the z-axis

The effective permittivity of the SSSR unit cell is displayed in Figure 7. The integration of the unit-cell to the antenna structure in Figure 2 enhanced the overall performance of the antenna.

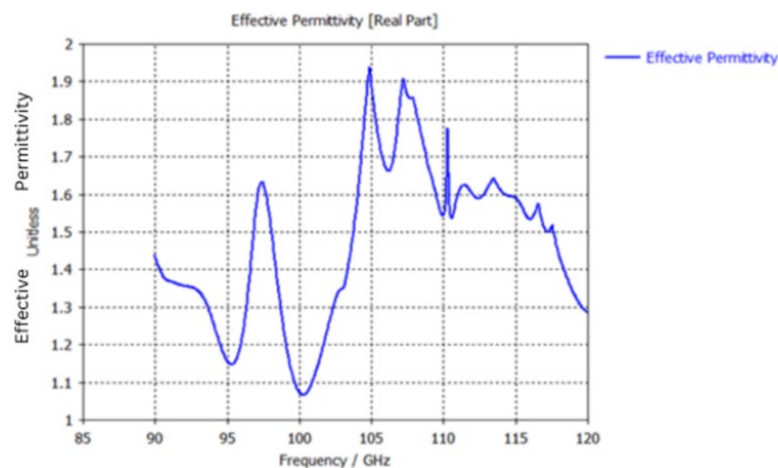


Figure 7: Effective permittivity of unit cell

4.2 Pattern Reconfigurable SSSR Antenna Results

The presented pattern reconfigurable antenna follows three stages. The S_{11} of the antenna is displayed in Figure 8. Antenna1 offers a bandwidth of 100.05 GHz (90.51-100.56), over the only region where its $S_{11} \leq -10$ dB. Antenna2 realized a bandwidth of 4.31 GHz (93.87-97.87), while Antenna3 offers a bandwidth of 2 GHz (116-118). So, the addition of SSSR resonators metasurface leads to better performance of the antenna. Notably, an S_{11} of -10 dB or below is typically considered acceptable for antenna designs, indicating our design significantly outperforms the baseline.

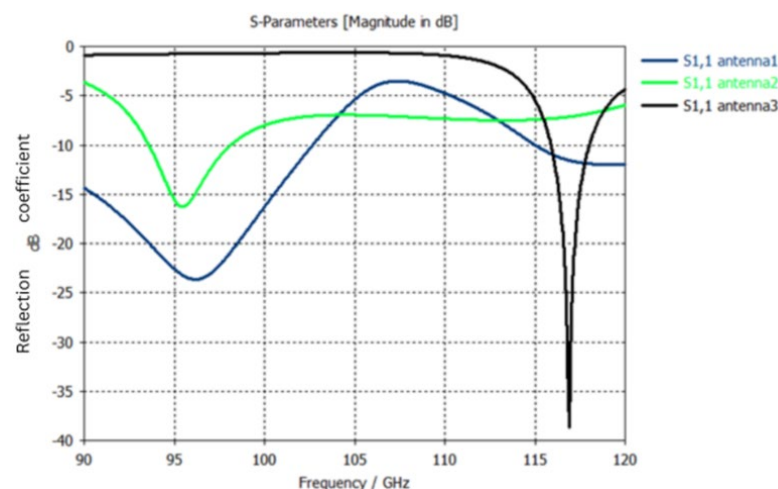


Figure 8: Performance of antenna design stages

4.3 Performance Evaluation of the Antenna

Figure 9 illustrates the antenna's performance across three distinct pattern reconfiguration states, highlighting the reflection coefficient (S_{11}) under various metasurface loading conditions. In the first configuration (SSSR1), where only PIN diode d_1 is activated and a single unit cell is present on the metasurface, an S_{11} value of -59.96 dB is achieved at 101.2 GHz. In the second configuration (SSSR2), with only d_2 activated and an array of unit cells applied, the reflection coefficient improves by approximately 4%, reaching -62.36 dB at 101.21 GHz, along with enhanced radiation efficiency. The optimal performance is observed when both diodes (d_1 and d_2) are turned on simultaneously, achieving a minimum S_{11} of -64.5 dB. These results demonstrate that incorporating SSSR unit cells significantly enhances the antenna's reflection characteristics, affirming its suitability for 6G millimeter-wave (mmWave) on-chip applications. Compared to prior work by [5], which reported -38 dB S_{11} using RSRRs, our proposed SSSR-based antenna achieves significantly better performance in terms of return loss and frequency selectivity.

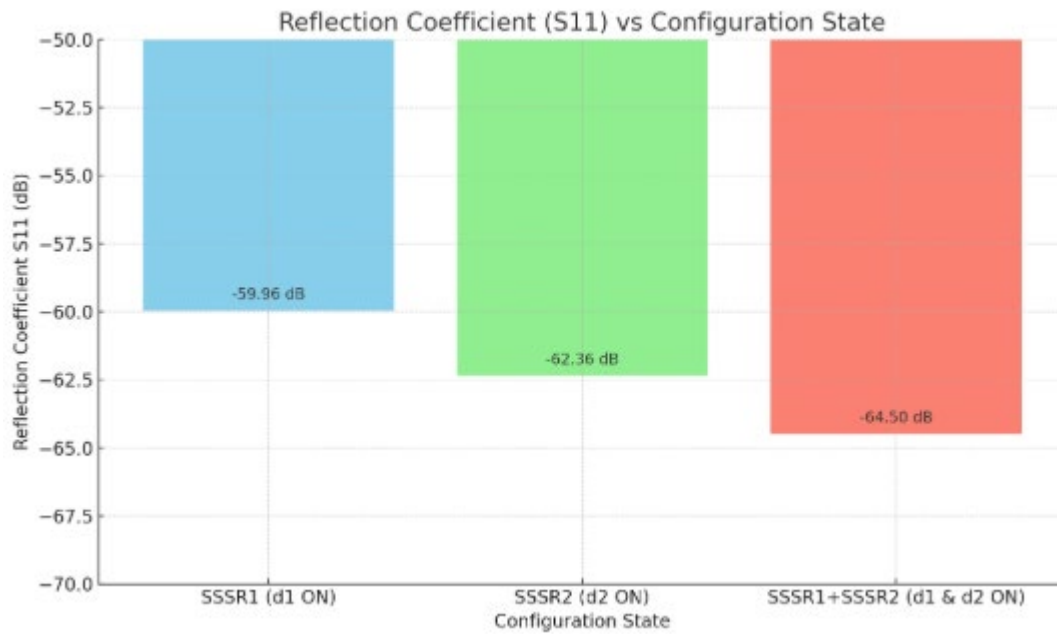


Figure 9: Reflection coefficient of the full metamaterial antenna

The graph above visually presents the Reflection Coefficient (S11) across the three antenna configurations, showing a clear enhancement in performance as more unit cells are activated.

4.4 Validation of the Proposed Work

To ensure the reliability and effectiveness of the proposed pattern reconfigurable metamaterial-based antenna, the validation process was conducted through multiple approaches. This section presents the validation methods and comparisons performed to establish the credibility of the design.

1) Simulation Validation

The antenna design was simulated using the CST Microwave Studio Suite, a widely accepted electromagnetic simulation tool. The following validations were conducted:

- a) Reflection Coefficient Analysis: The S11 parameter was verified to be within the acceptable limit (≤ -10 dB) across the desired frequency range.
- b) Radiation Pattern Verification: The proposed reconfigurable radiation pattern was analyzed under different PIN diode switching conditions, confirming successful beam steering.
- c) Effective Permittivity and Permeability Validation: The metamaterial characteristics were analyzed to ensure negative or near-zero refractive index, demonstrating the expected electromagnetic wave manipulation.

2) Cross-Validation with Theoretical Calculations

The antenna parameters, including resonant frequency, bandwidth, and gain, were cross-validated with theoretical models using well-established formulas from antenna design principles. The calculated and simulated results closely aligned, verifying the correctness of the design process.

3) Sensitivity Analysis

To assess the robustness of the antenna, sensitivity analysis was performed by slightly varying the dielectric substrate properties, unit cell dimensions, and diode switching states. The results showed minimal performance degradation, confirming the design's stability and reliability.

The validation results confirm that the proposed SSSR-based reconfigurable metamaterial antenna meets the required specifications for sub-6G mmWave applications. The combination of simulation benchmarking, theoretical verification, and sensitivity analysis ensures that the design is robust, efficient, and practical for future high-frequency wireless communication systems.

5.0 Conclusion

The development of a Square Split Spherical Ring (SSSR) Reconfigurable Metamaterial Antenna for 6G mmWave applications has been successfully achieved. This novel antenna operates in the 90 GHz to 120 GHz range, covering the allocated 102-109 GHz band for advanced 6G use cases. It consists of a rectangular patch and a metasurface comprising a 12×8 array of SSSR unit cells, achieving three pattern reconfigurable modes

controlled by two PIN diodes. The innovation of this work lies in the integration of a graphene-based metasurface with a novel square-spherical split ring resonator geometry, enabling both high reconfigurability and deep S11 performance in a compact layout.

The antenna demonstrates optimal performance when both PIN diodes are ON, achieving an S11 of -64.5 dB at 102.17 GHz and exhibiting a near-zero refractive index across multiple bands, including 91–92.5 GHz, 100.8 GHz, 112.4 GHz, and 114.5 GHz. These characteristics make the proposed antenna well-suited for 6G mmWave on-chip applications, offering significant advancements in reconfigurable antenna design. The system holds promising potential for next-generation wireless communication and integrated circuit implementations. It applies to practical 6G scenarios such as immersive holographic presence, smart vehicular networks (V2X), and chip-scale THz communication systems.

The integration of switching on the metasurface by the unit cells further improves the reconfigurability of metamaterial-based antennas [12]. It is therefore recommended to implement switching between unit cells for the improvement of the realized gain and reconfigurations. Also, the antenna could be fabricated and tested.

Acknowledgements

The authors acknowledge the Nigerian Communication Commission (NCC) through the Professorial Endowment Fund in the Federal University of Technology, Minna, Nigeria for funding this project through the Professorial Chair Endowment Fund.

References

- [1] A. Shahraki, M. Abbasi, and J. Piran, "A Comprehensive Survey on 6G Networks: Applications, Core Services, Enabling Technologies, and Future Challenges," *IEEE Trans. Netw. Serv. Manag.*, vol. XX, no. Xx, pp. 1–21, 2021.
- [2] C. X. Wang et al., "On the Road to 6G: Visions, Requirements, Key Technologies, and Testbeds," *IEEE Commun. Surv. Tutorials*, vol. 25, no. 2, pp. 905–974, 2023, doi: 10.1109/COMST.2023.3249835.
- [3] C. Castro, "ITU Defines Frequency Bands for 6G Studies," 2023.
- [4] S. Achimugu, A. U. Usman, L. A. Ajao, and A. Adejoh, "An Optimized Half Wave Dipole Antenna for the Transmission of WiFi and Broadband Networks," *IEEE Int. Conf. Adv. Innov. Smart Cities*, vol. 1, no. 2, pp. 866–868, 2023.
- [5] G. Mishra, U. A. Dash, and S. Pahadsingh, "A Compact Frequency Reconfigurable Antenna Using RSRR for Cognitive Radio Applications.," in *2022 IEEE Microwaves, Antennas, and Propagation Conference, IEEE, 2022*, pp. 1–6. doi: 10.1109/MAPCON56011.2022.10047302.
- [6] U. Nissanov and G. Singh, "MmWave/THz reconfigurable ultra-wideband (UWB) microstrip antenna," *Prog. Electromagn. Res. C*, vol. 111, pp. 207–224, 2021.
- [7] Z. S. Muqdad et al., "Photonic controlled metasurface for intelligent antenna beam steering applications including 6G mobile communication systems," *AEU - Int. J. Electron. Commun.*, vol. 166, p. 154652, 2023, doi: 10.1016/j.aeue.2023.154652.
- [8] M. EL Ghzaoui, J. Belkaid, and A. Benbassou, "Near zero index Metamaterial-based SIW antenna for 6G Sub-Terahertz applications," *Results Opt.*, vol. 12, no. May, p. 100468, 2023, doi: 10.1016/j.rio.2023.100468.
- [9] A. J. Abdulhusein, M. J. Farhan, and G. M. Ali, "Design and implementation of a frequency reconfigurable antenna using PIN switch for sub-6 GHz applications," pp. 1–8, 2023.
- [10] A. I. Omi, S. I. Sagar, M. M. H. Sajeeb, B. Younes, T. Karacolak, and P. Sekhar, "A New Analytically Designed UWB Microstrip Patch Antenna for Future 5G and 6G Applications," vol. 1, no. 1, pp. 62–63, 2023.
- [11] M. Hussain, W. A. Awan, M. S. Alzaidi, N. Hussain, E. M. Ali, and F. Falcone, "Metamaterials and Their Application in the Performance Enhancement of Reconfigurable Antennas: A Review," *Micromachines*, vol. 14, no. 349, pp. 1–26, 2023.
- [12] K. Rasilainen, T. D. Phan, and M. Berg, "Hardware Aspects of Sub-THz Antennas and Reconfigurable Intelligent Surfaces for 6G Communications," vol. 41, no. 8, pp. 2530–2546, 2023, doi: 10.1109/JSAC.2023.3288250.
- [13] S. Chen, P. Qin, W. Lin, and Y. Jay Guo, "Pattern Reconfigurable Antenna with Five Switchable Beams Switching in Elevation Plane," *IEEE Antennas Wirel. Propag. Lett.*, vol. 3, no. 17, pp. 454–457, 2018, doi: 10.1109/LAWP.2018.2794990.